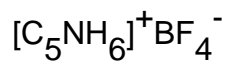


Thermodynamics of the phase transitions in ferroelectric pyridinium tetrafluoroborate



This article has been downloaded from IOPscience. Please scroll down to see the full text article.

2000 J. Phys.: Condens. Matter 12 643

(<http://iopscience.iop.org/0953-8984/12/5/312>)

View [the table of contents for this issue](#), or go to the [journal homepage](#) for more

Download details:

IP Address: 171.66.16.218

The article was downloaded on 15/05/2010 at 19:40

Please note that [terms and conditions apply](#).

## Thermodynamics of the phase transitions in ferroelectric pyridinium tetrafluoroborate $[\text{C}_5\text{NH}_6]^+\text{BF}_4^-$

Izabela Szafraniak<sup>†</sup>, Piotr Czarnecki<sup>†</sup> and Peter U Mayr<sup>‡</sup>

<sup>†</sup> Institute of Physics, Adam Mickiewicz University, Umultowska 85, 61-614 Poznań, Poland

<sup>‡</sup> Abteilung Angewandte Physik, University of Ulm, D-89069 Ulm, Germany

E-mail: izaszaf@main.amu.edu.pl

Received 28 July 1999, in final form 3 November 1999

**Abstract.** The anomaly of specific heat at the phase transitions was studied by differential scanning calorimetry (DSC) and the anisotropy of linear thermal expansion was studied by dilatometry on monocrystals of pyridinium tetrafluoroborate  $[\text{C}_5\text{NH}_6]^+\text{BF}_4^-$ . The effect of hydrostatic pressure on the phase transitions was studied by the methods of pressure dilatometry and pressure DTA. We found that the temperature of ferroelectric phase transition at  $T_1 = 238$  K as well as the temperature of non-ferroelectric phase transition at  $T_2 = 204$  K increase with pressure. The thermodynamic parameters determined on the basis of the calorimetric measurements are consistent with those obtained from the Ehrenfest relationship for second order phase transitions. The pressure experiments allowed us to construct the  $p$ - $T$  phase diagram up to 300 MPa. We estimated the uniaxial pressure dependence of the phase transition temperature. The mechanism of both phase transitions is proposed.

### 1. Introduction

The discovery of ferroelectric properties in certain pyridinium salts at the beginning of the 1990s aroused a new great interest in this group of compounds [1]. The majority of these salts crystallize in the trigonal system  $R\bar{3}m$  or  $R3m$  [2–4], in which the planar pyridinium cations are arranged in parallel (figure 1). Characteristic of this family of crystals are fast jumps of the pyridinium cations about the pseudohexagonal symmetry axis occurring at room temperature. In the high-temperature phase, position symmetry of the cation in a trigonal cell implies cation reorientations among the equivalent potential barriers. With decreasing temperature the cation dynamics changes, which results in the occurrence of phase transitions. At low temperatures the cation reorientates among inequivalent potential barriers. The majority of pyridinium salts reveal one phase transition, though the ferroelectric salts (pyridinium tetrafluoroborate, pyridinium perchlorate, pyridinium periodate and pyridinium perrhenate, denoted  $\text{PyBF}_4$ ,  $\text{PyClO}_4$ ,  $\text{PyIO}_4$ ,  $\text{PyReO}_4$ , respectively) undergo a sequence of two phase transitions [1, 5–7]. The additional transition taking place at higher temperature is ferroelectric. The compounds show a variety of physical properties; their phase transitions differ in character, entropy change at the phase transition, the effect of hydrostatic pressure. Results of dielectric measurements performed for the oriented single crystal samples of  $\text{PyBF}_4$  revealed the ferroelectric properties along the three twofold axes of the trigonal system. According to the earlier studies,  $\text{PyBF}_4$  shows two continuous phase transitions at  $T_1 = 238$  K and at  $T_2 = 204$  K and the sequence of

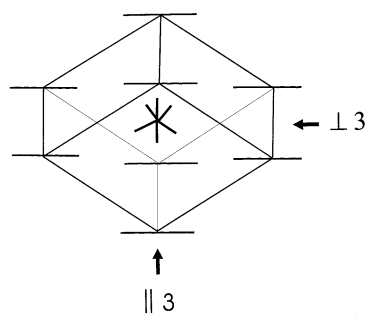


**Figure 1.** Schematic unit cell of  $\text{PyBF}_4$  in the high-temperature phase. The bold lines represent the pyridinium cations; in the middle of the unit cell is the disordered  $\text{BF}_4^-$  anion. The two most anisotropic directions—along and perpendicular to the threefold axis—are denoted as  $\parallel 3$  and  $\perp 3$  respectively.

structural phase transition is  $R\bar{3}m \xrightarrow{238\text{ K}} C2 \xrightarrow{204\text{ K}} P2$  [4].  $\text{PyBF}_4$  is a unique example of a multiaxial ferroelectric undergoing a continuous phase transition [4].

Pyridinium cations have permanent dipole moments and, in the high-temperature phase, the resultant moment is zero because of fast reorientations. The directions of the spontaneous polarization vector coincide with those of the dipole moment of the cations, but the ferroelectric properties of  $\text{PyBF}_4$  are not determined only by the change in the cation disorder. Because of the planar arrangement of the cation in the crystal lattice, the greatest anisotropy of physical properties is expected in the directions along and perpendicular to the threefold symmetry axis of the trigonal system (figure 1). So far the anisotropies of dielectric properties in single crystals of  $\text{PyBF}_4$  and  $\text{PyClO}_4$  have been described [4, 8].  $\text{PyBF}_4$  belongs to a group of ionic-molecular crystals in which even small changes of hydrostatic pressure can induce significant changes in interionic distances and interactions. The aim of this work has been to establish the effect of hydrostatic pressure on the phase transitions in  $\text{PyBF}_4$ . Results of our measurements enabled a construction of phase diagrams and their analysis on the basis of the Ehrenfest equation as well as determination of thermodynamic parameters of the phase transitions. Moreover, anisotropy of the linear expansion of  $\text{PyBF}_4$  has been discussed and its analysis allowed evaluation of the effect of uniaxial pressure on the phase transition temperatures.

## 2. Experiment

The  $\text{PyBF}_4$  salt is formed in the reaction between pyridine and tetrafluoroboric acid. Prior to measurements, the substance was recrystallized three times.  $\text{PyBF}_4$  crystals were grown from a water solution by slow evaporation at a constant temperature. The maximum size of the rhombohedral crystals was  $10 \times 10 \times 10 \text{ mm}^3$ . Small single crystal samples were used for calorimetric measurements, whereas for measurements of linear expansion we used samples cut out of the single crystals as rectangular prisms oriented along the threefold axis of the trigonal system or perpendicular to it. Measurements of volumetric thermal expansion under ambient and high pressure were carried out for polycrystalline samples, pressed into cylinders of 5.8 mm in diameter and 10 mm in length.

Differential scanning calorimetry (DSC) measurements were carried out on a Perkin–Elmer DCS-2 in the temperature range from 160 to 290 K, at a heating rate of  $10 \text{ K min}^{-1}$ .

High-pressure differential thermal analysis (DTA) measurements were made for a few values of hydrostatic pressure from the range 50–300 MPa. The high-pressure chamber was connected to a gas compressor GCA-10 made by Unipress. Pressure was established with the accuracy of  $\pm 2 \text{ MPa}$ . Temperature was changed at the rate of  $5 \text{ K min}^{-1}$ . The experimental setup has been described in [9].

The specific volume and the linear thermal expansion of the crystal were measured with a Netzsch dilatometer in the temperature range from 170 to 300 K at the heating rate of 0.5 or 1  $\text{K min}^{-1}$ . The influence of hydrostatic pressure on the specific volume of the crystal was tested by pressure–volume dilatometry on self-developed equipment [10, 11]. Isobaric measurements of the specific volume were performed for a few chosen pressure values from the range 10–100 MPa and isothermal measurements for a few chosen temperatures from the range 230–300 K. For the isobaric measurements the rate of temperature change was 0.5  $\text{K min}^{-1}$ , while for the isothermal measurements the rate of pressure change was 10  $\text{MPa min}^{-1}$ . The measurements were carried out in a high-pressure chamber filled with silicon oil. As the silicon oil freezes at about 230 K, measurements below this temperature could not be performed.

### 3. Results

#### 3.1. DSC measurements

Two runs of measurements were made and a remarkable repeatability of results was achieved. The temperature dependence of specific heat is shown in figure 2, and reveals two anomalies related to the phase transitions at  $T_1 = 238 \text{ K}$  and  $T_2 = 204 \text{ K}$ . The character of these anomalies is typical of continuous phase transitions. No temperature hysteresis is observed. No anomalous changes in specific heat  $C_p$  are observed from the high-temperature side, which means that the order parameter fluctuations do not play an essential role in this phase transition, as if they did they would force the first order phase transition [12]. The entropy change at the phase transition significantly depends on the choice of the baseline and the range of integration. The total change of entropy (figure 2) determined from the above measurements varies from  $\Delta S = 18$  to  $\Delta S = 24 \text{ J K}^{-1} \text{ mol}^{-1}$ , depending on the choice of the baseline. It is very difficult to establish the accurate change of entropy in particular transitions, because of small temperature differences between them. The pretransitional effects of continuous transitions may start as early as a few tens of kelvin below the phase transition temperature. These

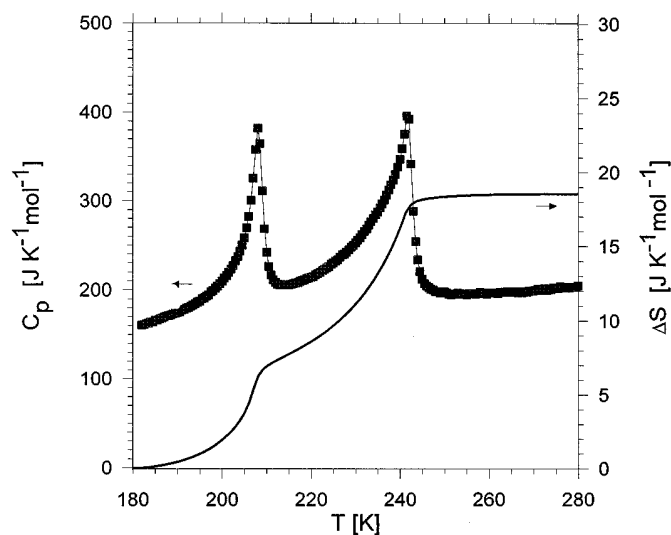


**Figure 2.** The temperature dependence of specific heat  $C_p$  (left) and the entropy change  $\Delta S$  (right).

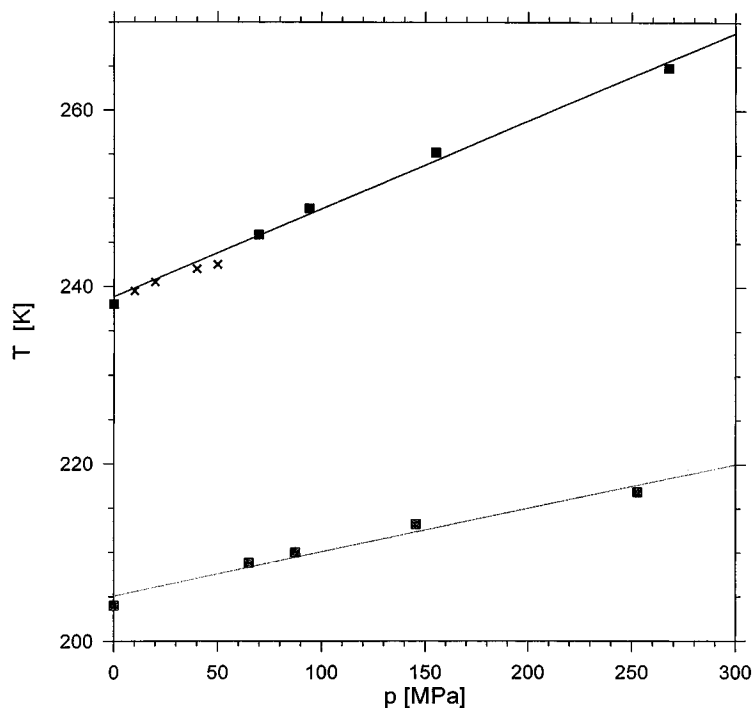


**Figure 3.** The  $p$ - $T$  phase diagram of  $\text{PyBF}_4$  obtained from DTA (squares) and dilatometric measurements (crosses).

relatively small effects bring, however, a significant contribution to the total change of entropy. The change of entropy  $\Delta S_1$  at ferroelectric phase transition  $T_1$  varies from 11 to 15  $\text{J K}^{-1} \text{mol}^{-1}$  and at  $T_2$  from 5.5 to 9.5  $\text{J K}^{-1} \text{mol}^{-1}$ .

### 3.2. High-pressure DTA measurements

DTA measurements were carried out for a few chosen values of hydrostatic pressure from the range 50–300 MPa. With increasing pressure, the temperatures of anomalies related to the phase transitions shift toward higher values. A decrease in the anomaly of the DTA signal for higher pressures is a result of a decrease in the apparatus sensitivity [9]. The anomaly of the DTA signal, typical of continuous phase transitions, does not change its character in the pressure range studied. The phase diagram obtained for  $\text{PyBF}_4$  is shown in figure 3. As follows from the data, the temperature of phase transitions shows linear changes with pressure, and the relevant dependences can be expressed as:

$$T_1(p) = 238 + p \times 106 \text{ K GPa}^{-1} \text{ for the ferroelectric phase transition, and}$$

$$T_2(p) = 204 + p \times 45 \text{ K GPa}^{-1} \text{ for the low-temperature phase transition.}$$

### 3.3. Dilatometric measurements

Measurements of the thermal linear expansion were performed in the two most anisotropic directions—along the threefold axis and perpendicular to it. The temperature dependence of linear expansion is shown in figure 4. In the vicinity of phase transitions the crystal length

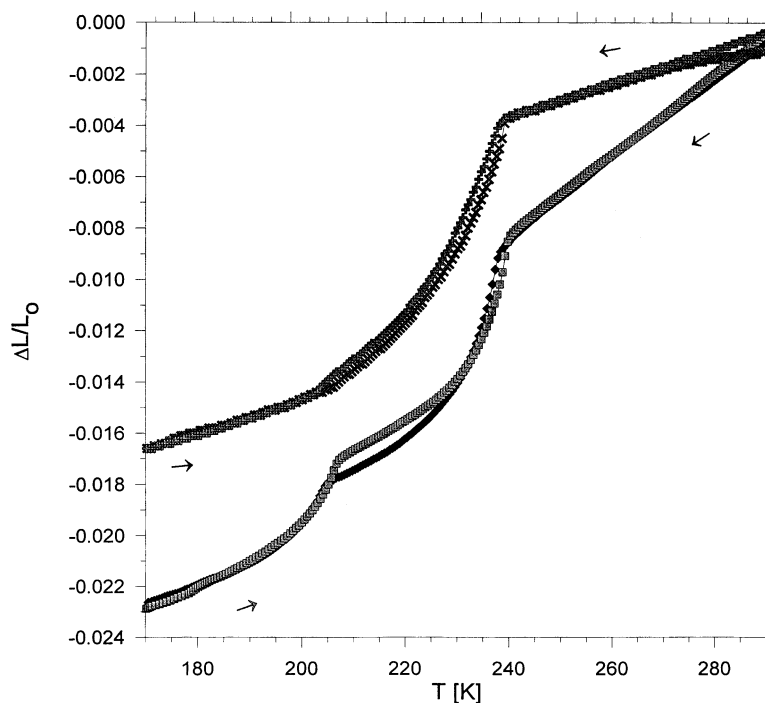


**Figure 4.** The temperature dependence of the linear thermal expansion  $\Delta l/l_0$  measured along (squares) and perpendicular (crosses) to the threefold axis obtained on heating and cooling. The cooling and the heating runs are denoted by arrows.

changes linearly. The changes are the most pronounced in the direction parallel to the threefold axis, so perpendicular to the pyridinium ring planes. This anisotropy follows from the structure and is probably a result of the planar arrangement of the cations in the crystal lattice. The changes are easier in the direction perpendicular to the planar pyridinium cations. At the low-temperature phase transition in the direction perpendicular to the threefold axis the change in the crystal length is barely detectable, which is caused by the fact that at this transition main changes occur along the threefold axis, so in the distances between the pyridinium planes. The linear expansion coefficient  $\alpha_l = (1/l)(\partial l/\partial T)_p$  was calculated, and its temperature dependence is shown in figure 5.

Results of the volumetric thermal expansivity measurements carried out for polycrystalline samples are given in figure 6. The temperature dependence of the volumetric expansivity  $\alpha_V = (1/V)(\partial V/\partial T)_p$  is shown in figure 6.

### 3.4. High-pressure dilatometric measurements

The temperature dependence of the volume thermal expansion for a few values of hydrostatic pressure is presented in figure 7. The phase transition temperature increases with increasing pressure, but the character of the anomaly in the vicinity of the phase transition does not change in the pressure range studied. The pressure dependence of the temperature of the phase transition  $T_1$  is shown in the  $p$ - $T$  phase diagram (see figure 3). The results of the isothermal studies are given in figure 8 and the compressibility  $\beta = (1/V)(\partial V/\partial T)_p$  is equal to  $1.4 \times 10^{-10} \text{ Pa}^{-1}$ .

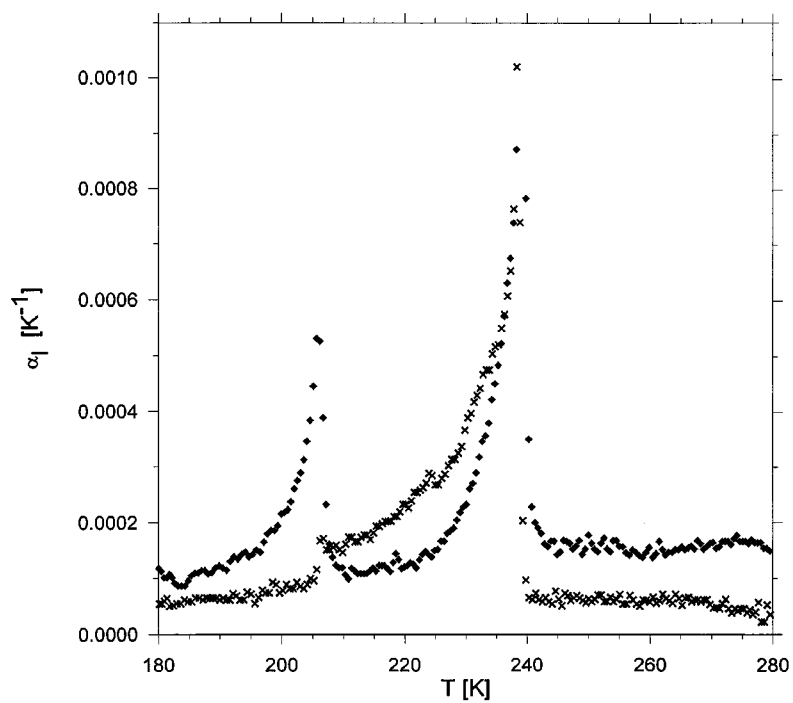


**Figure 5.** The temperature dependence of the linear thermal expansivity  $\alpha_l$  measured along (squares) and perpendicular (crosses) to the threefold axis.

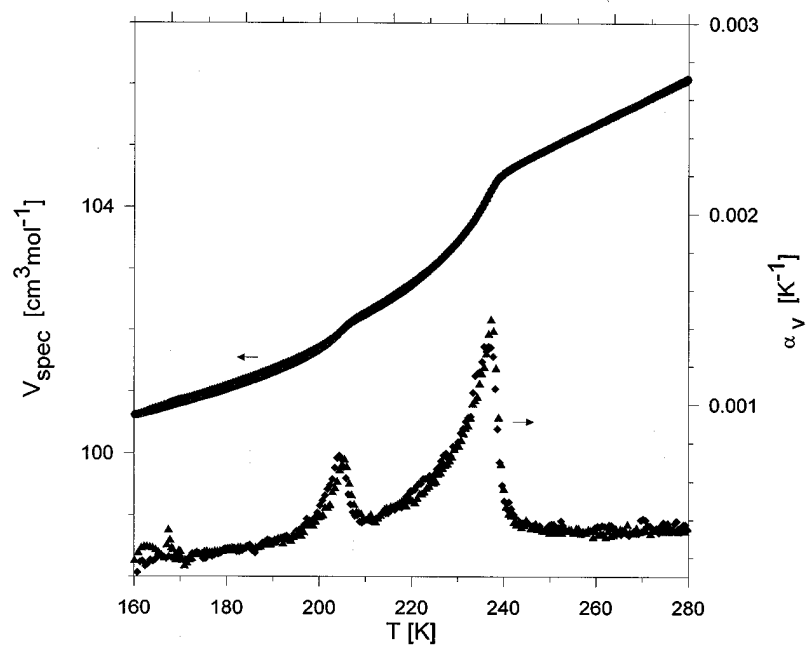


**Figure 6.** The temperature dependence of the specific volume (left) and the volumetric thermal expansivity  $\alpha_v$  (right) obtained on heating and cooling at the rate of  $1 \text{ K min}^{-1}$ .

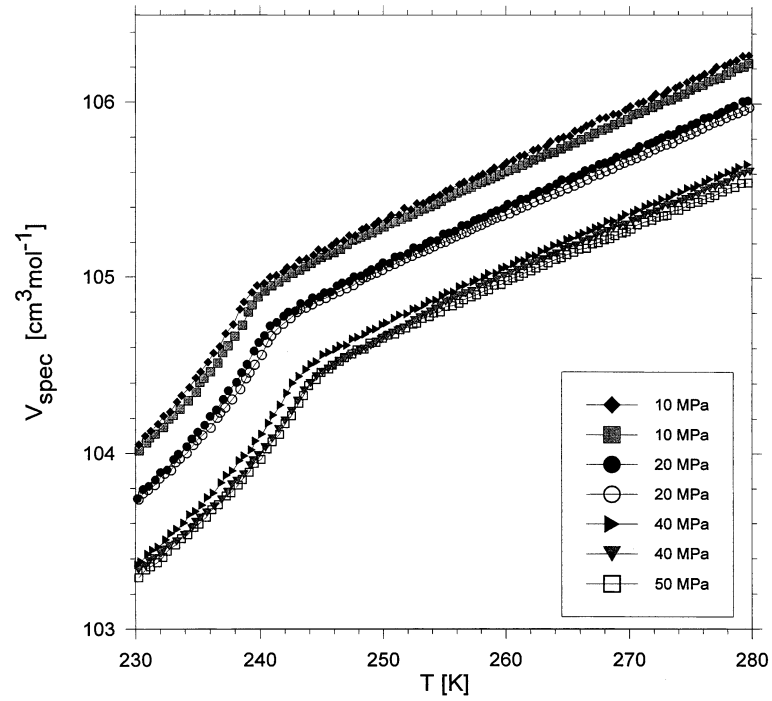


**Figure 7.** The temperature dependence of the specific volume under hydrostatic pressure obtained during cooling and heating.

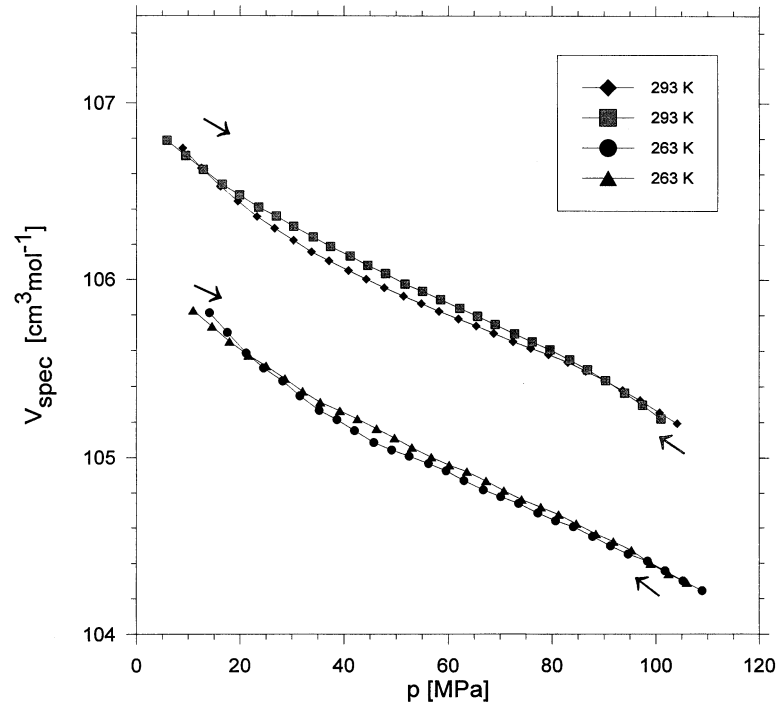


**Figure 8.** The specific volume versus hydrostatic pressure. The increasing and the decreasing runs of pressure are denoted by arrows.



#### 4. Discussion

Results of the x-ray and neutron diffraction studies performed for strongly disordered structures do not permit exact determination of the number of reorientation positions of ions in particular phases. From structural studies [4] it is known that in the high-temperature phase the pyridinium cation rotates about the pseudohexagonal symmetry axis and the  $\text{BF}_4$  anion is strongly disordered. A large total entropy change accompanying the phase transitions indicates a change in the dynamics of ions. Knowing the change of entropy  $\Delta S$ , the change in the number of inequivalent positions can be estimated from the relation:

$$\Delta S = R \ln N_1/N_2$$

where  $N_1$  and  $N_2$  are the numbers of inequivalent positions in the high- and low-temperature phase and  $R$  is the gas constant. The total change of entropy is about  $\Delta S = 22 \text{ J K}^{-1} \text{ mol}^{-1}$ , which is close to  $\Delta S = R \ln 12$ , so  $N_1/N_2 = 12$ . Thus, at room temperature, the pyridinium cation can take six inequivalent positions. This number is typical of other pyridinium salts of the same structure, like pyridinium iodide PyI and pyridinium hexafluorophosphate  $\text{PyPF}_6$ , [13, 14]. In the low-temperature phase the cation reorientations stop. The number of cation positions in the low-temperature phase has not been determined, but it is reasonable to suppose that the phase is ordered and the number of possible cation positions is 1. In the high-temperature phase, the anion performs reorientations, which slow down with decreasing temperature.

It seems most probable that at the Curie point the entropy change is  $\Delta S_1 = R \ln 4$ , while at the low-temperature phase transition  $\Delta S_2 = R \ln 3$ . Assuming these values, the mechanism of the phase transition may be as follows: at the Curie point the pyridinium cation begins to perform jumps among three positions ( $\Delta S = R \ln 6/3 = R \ln 2$ ). A change in the cations motion induces a change in the anions reorientations. The number of inequivalent positions of the anion is twice reduced. The entropy change related to the change in the anion dynamics is  $\Delta S = R \ln 2$ . At the low-temperature phase transition the cation dynamics changes. Instead of three positions in the intermediate phase it has only one position in the low-temperature phase. At this phase transition the change in entropy related to the change of the cation dynamics is  $\Delta S_2 = R \ln 3/1$ . The change in the  $\text{BF}_4$  anion dynamics does not contribute to the change in entropy.

Assuming the same total change in entropy  $\Delta S = R \ln 12$ , an alternative mechanism of phase transitions can be given. At the Curie point, the entropy can change by  $\Delta S_1 = R \ln 6$ , while in the low-temperature phase  $\Delta S_2 = R \ln 2$ . Assuming these values, the mechanism of the phase transitions can be as follows: below the Curie point the pyridinium cation is completely ordered and the number of possible cation positions is 1 ( $\Delta S_1 = R \ln 6/1$ ). At the low-temperature phase transition the anion stops at one of two possible positions ( $\Delta S_2 = R \ln 2/1$ ). The most probable to us is the former mechanism, because in phase II there are still reorientations of cations [15].

The values of  $\Delta C_p$  from calorimetric measurements and  $\Delta \alpha_V$  from dilatometric measurements (see table 1) were used to obtain the pressure dependence of the phase transition temperatures, from the Ehrenfest relation:

$$\frac{\partial T_0(p)}{\partial p} = T_0(p=0) \frac{\Delta \alpha_V V_m}{\Delta C_p}$$

where  $\Delta C_p$  is the specific heat jump at  $T_0$  and  $V_m$  is the molar volume.

The values of  $\partial T_1/\partial p = 138 \text{ K GPa}^{-1}$  and  $\partial T_2/\partial p = 46 \text{ K GPa}^{-1}$ , determined for the high- and low-temperature transitions, respectively, are consistent with those found from the phase diagram.

**Table 1.** Thermodynamic parameters of the phase transitions.

	204 K	238 K
Density	$9.8 \times 10^3 \text{ mol m}^{-3}$	$9.6 \times 10^3 \text{ mol m}^{-3}$
Jump of $C_p$	$170 \text{ J K}^{-1} \text{ mol}^{-1}$	$190 \text{ J K}^{-1} \text{ mol}^{-1}$
Jump of $\alpha_V$	$4 \times 10^{-4} \text{ K}^{-1}$	$11 \times 10^{-4} \text{ K}^{-1}$
Jump of $\alpha_{\parallel}$	$3.6 \times 10^{-4} \text{ K}^{-1}$	$9.3 \times 10^{-4} \text{ K}^{-1}$
Jump of $\alpha_{\perp}$	$-0.6 \times 10^{-4} \text{ K}^{-1}$	$8.3 \times 10^{-4} \text{ K}^{-1}$

The magnitude and signs of the  $\Delta\alpha_i$  values provide information about the uniaxial pressure dependence of  $T_0$  via Ehrenfest relationship:

$$\frac{\partial T(p)}{\partial p_i} = T_0(p=0) \frac{\Delta\alpha_i V_m}{\Delta C_p}$$

The uniaxial  $\partial T_0/\partial p_i$  values calculated from our data are thus:  $\partial T_1/\partial p_{\perp} = +96 \text{ K GPa}^{-1}$  and  $\partial T_1/\partial p_{\parallel} = +108 \text{ K GPa}^{-1}$  for the high-temperature phase transition and  $\partial T_2/\partial p_{\perp} = -8 \text{ K GPa}^{-1}$  and  $\partial T_2/\partial p_{\parallel} = +44 \text{ K GPa}^{-1}$  for the low-temperature phase transition. We found that  $\partial T_2/\partial p_{\perp}$  is negative and  $\partial T_2/\partial p_{\parallel}$  is positive for the low-temperature phase transition. A detailed investigation of the effect of uniaxial pressure on the temperature of phase transition is under way.

## 5. Conclusions

As follows from the character of anomalies established in calorimetric and dilatometric studies, phase transitions in PyBF<sub>4</sub> are continuous.

The phase transitions in PyBF<sub>4</sub> are of the order–disorder type, in which the dynamics of both cations and anions changes.

The phase diagram constructed indicates that the pressure dependences of the phase transition temperatures are in agreement with the Ehrenfest relation.

The anisotropy of linear expansion is a consequence of the crystal structure. The low-temperature phase transition is related first of all to the change in the distance between the pyridinium planes.

The uniaxial pressure dependence of the phase transition temperature is highly anisotropic.

## Acknowledgments

The authors wish to express thanks to Anne-Marie Saier for her help during dilatometric measurements and Dr G W H Höhne for his help in DSC measurements.

The present work has been supported by the Polish Scientific Research Committee (KBN) under grant 2P03B00816.

## References

- [1] Czarnecki P, Nawrociak W, Pająk Z and Wąsicki J 1994 *Phys. Rev. B* **49** 1511
- [2] Copeland R F, Conner S H and Meyers E A 1966 *J. Phys. Chem.* **70** 1288
- [3] Hartl H 1975 *Acta Crystallogr. B* **31** 1781
- [4] Czarnecki P, Katrusiak A, Szafraniak I and Wąsicki J 1998 *Phys. Rev. B* **57** 3326
- [5] Czarnecki P, Nawrociak W, Pająk Z and Wąsicki J 1994 *J. Phys. C: Solid State Phys.* **6** 4955
- [6] Wąsicki J, Czarnecki P, Pająk Z, Nawrociak W and Szczepański W 1997 *J. Chem. Phys.* **107** 576

- [7] Pająk Z, Czarnecki P, Wąsicki J and Nawrocik W 1998 *J. Chem. Phys.* **109** 6420
- [8] Czarnecki P, Wąsicki J, Pająk Z, Goc R, Małuszyńska H and Habryło S 1997 *J. Mol. Struct.* **404** 175
- [9] Szafranski M, Czarnecki P, Katrusiak A and Habryło S 1992 *Solid State Commun.* **82** 277
- [10] Dollhopf W, Barry S and Strauss M J 1991 *Frontiers of High-Pressure Research* ed H D Hochheimer and R D Ethers (New York: Plenum) pp 25–32
- [11] Höhne G W H, Dollhopf W, Blankenhorn K and Mayr P U 1996 *Thermochim. Acta* **273** 17
- [12] Strukov B A and Levanyuk A P 1983 *Fizicheskie Osnovy Segnetoelektricheskikh Yavleni v Kristalakh* (Moscow: Nauka) pp 129–31
- [13] Lewicki S, Wąsicki J, Czarnecki P, Szafraniak I, Kozak A and Pająk Z 1998 *Mol. Phys.* **94** 973
- [14] Szafraniak I, Czarnecki P, Mayr P U and Dollhopf W 1999 *Phys. Status Solidi b* **213** 15
- [15] Czarnecki P and Szafraniak I 1998 *Phys. Status Solidi b* **209** 211